



Available online at www.sciencedirect.com

ScienceDirect

Food Science and Human Wellness xxx (2016) xxx–xxx

Food Science
and Human Wellness

www.elsevier.com/locate/fshw

Biological activities of silver nanoparticles from *Nothapodytes nimmoniana* (Graham) Mabb. fruit extracts

G. Mahendran, B.D. Ranjitha Kumari *

Department of Plant Science, School of Life Sciences, Bharathidasan University, Tiruchirappalli, 620 024 Tamil Nadu, India

Received 29 September 2015; received in revised form 27 September 2016; accepted 8 October 2016

Abstract

In the present investigation, we have described the green biosynthesis of silver nanoparticles (AgNPs) using ripened fruit aqueous extract of *Nothapodytes nimmoniana* (Graham) Mabb. as capping agent. The antioxidant, anticancer and antimicrobial activities of AgNPs were also studied. UV analysis revealed that AgNPs had a sharp peak at 416 nm. X-ray diffraction (XRD) result confirmed the characteristic peaks indicated at 111, 200, 220 and 311 for the crystalline of the face centered cubic silver. The Scanning Electron Microscopy analysis results confirmed the spherical shaped of AgNPs with difference sizes of the particles and an average from 44 to 64 nm. Further, fruit extract and AgNPs were evaluated total phenolic, tannin and flavonoid contents and were subjected to assess their antioxidant potential using various *in vitro* systems such as using 1,1-diphenyl-2-picryl-hydrazyl (DPPH), 2,2'-azinobis-(3-ethylbenzothiazoline-6-sulfonic acid) (ABTS), metal chelating, phosphomolybdenum and ferric reducing antioxidant power (FRAP) activities and antimicrobial activity against *Bacillus subtilis*, *Pseudomonas aeruginosa*, *Klebsiella pneumoniae*, *Staphylococcus aureus* and *Escherichia coli*. When compared to AgNPs, fruit extract exhibited uppermost radical scavenging activities. In addition, the cytotoxicity activity was determined by MTT assay. Our results clearly proved that biosynthesized AgNPs inhibited proliferation of HeLa cell line with an IC₅₀ of 87.32 ± 1.43 µg/mL and antibacterial activity.

© 2016 Beijing Academy of Food Sciences. Production and hosting by Elsevier B.V. This is an open access article under the CC BY-NC-ND license (<http://creativecommons.org/licenses/by-nc-nd/4.0/>).

Keywords: Silver nanoparticles; Green synthesis; Cytotoxicity; Antioxidant; DPPH; FRAP; XRD; *Nothapodytes nimmoniana*

1. Introduction

Most of the oxidative diseases are due to oxidative stress resulting from free radicals [1]. Free radicals such as superoxide anion, hydroxyl radicals and non-radical species such as hydrogen peroxide and singlet oxygen are different varieties of activated oxygen constituting reactive oxygen species (ROS) [2,3]. An active antioxidative defense system is needed to balance the output of free themes. The oxidative damage pro-

duced by free radical generation is a critical etiological factor implicated in several chronic human diseases such as diabetes mellitus, cancer, atherosclerosis, arthritis and neurodegenerative diseases and also in the aging procedure. In the discussion of these diseases, antioxidant therapy has made an enormous importance [4].

Nowadays, the metal nanoparticles may act both as reducing agents by plant extracts and stabilizing agents in the synthesis of nanoparticles due to their specific electrical, optical, magnetic, chemical and mechanical properties are currently used in many high technology areas, such as the medical sector for imaging, faster diagnosis, drug delivery, tissue regeneration, cancer therapeutics, bactericidal and fungicidal agents and antioxidants, as well as the development of new therapeutics [5].

The synthesis of AgNPs can be achieved by chemical reduction [6], electrochemical [7], γ ray irradiation [8], UV-radiation therapy [9], photochemical reduction [10], ultrasonic assisted [11], microwave [12], and laser ablation [13,14]. But each

* Corresponding author at: Department of Plant Science, School of Life Sciences, Bharathidasan University, Tiruchirappalli, 620 024 Tamil Nadu, India. Fax: +91 4222422387.

E-mail address: ranjithakumari2004@yahoo.co.in (B.D. Ranjitha Kumari).

Peer review under responsibility of Beijing Academy of Food Sciences.



Production and hosting by Elsevier

<http://dx.doi.org/10.1016/j.fshw.2016.10.001>

2213-4530/© 2016 Beijing Academy of Food Sciences. Production and hosting by Elsevier B.V. This is an open access article under the CC BY-NC-ND license (<http://creativecommons.org/licenses/by-nc-nd/4.0/>).

method has been argued in the term of cost, scalability, particle size and dispersion. In particular, chemical method of nanoparticle synthesis was commonly used, but concerning about the adverse toxic effect to the environment, researchers were required to develop a green chemistry protocol for nanoparticle synthesis [15]. Nanoparticle synthesis through exploiting the bio resources (bacteria, fungi, yeasts, algae or plants) proves to be very feasible, cost-effective and eco-friendly alternate [16].

Numerous reports on the synthesis of AgNPs using fruit extract as environmentally friendly substitutes to chemical and physical methods. Further, the survey of earlier literatures suggests that fruit extracts from various plants such as *Terminalia chebula* [17], Banana (*Musa* sp.) [18], *Dillenia indica* [19], *Solanum lycopersicum* [20], *Emblica officinalis* [21], *Carica papaya* [22], *Crataegus douglasii* [23], *Garcinia mangostana* [24], *Averrhoa carambola* [25] and *Lantana camara* [26] are brimming a source for the synthesis of silver nanoparticles as an alternative to the conventional methods.

Considering the vast potentiality of plants as sources this work aims to apply a biological green technique for the synthesis of silver nanoparticles as an alternative to conventional methods. In this regard, *Nothapodytes nimmoniana* (Icacinaceae) is a small tree, naturally distributed in many parts of the Western Ghats. This tree is a rich source of camptothecin, isoquinoline alkaloid which is currently being used for treating colorectal and ovarian cancer [27]. Silver nanoparticles can be prepared with lower amounts of plant based extract and without any additional chemicals/and or physical steps [28]. Therefore, in the present study, we have synthesized silver nanoaprticles using an aqueous fruit extract of *N. nimmoniana* and evaluated for antioxidant, antimicrobial and anticancer potentials toward biomedical applications.

2. Materials and methods

2.1. Materials

All the chemicals and reagents used in this study were of analytical grade, silver nitrate (AgNO_3 , 99.9%) was obtained from Sigma-Aldrich Chemical Company. The fruit of *N. nimmoniana* were collected from Velliangiri hills, Coimbatore, Tamil Nadu during 2015. The identification of the plant material was done by Dr. M. Murugesan, Scientist B, Botanical survey of India, Eastern Regional Centre, Shillong, India.

2.2. Preparation of *N. nimmoniana* fruit extract

N. nimmoniana fruit extract (NN) was used as a reducing agent for the development of AgNPs. The fresh fruits of NN (Fig. 1) washed repeatedly with distilled water to remove the dust and organic impurities present in it and then dried on paper toweling. About 5 g of fruits was crushed into fine pieces with sterilized knife. The fruit of NN was taken into the 500 mL beaker containing 100 mL of double distilled water and then the solution was boiled for 10 min and filtered through What-

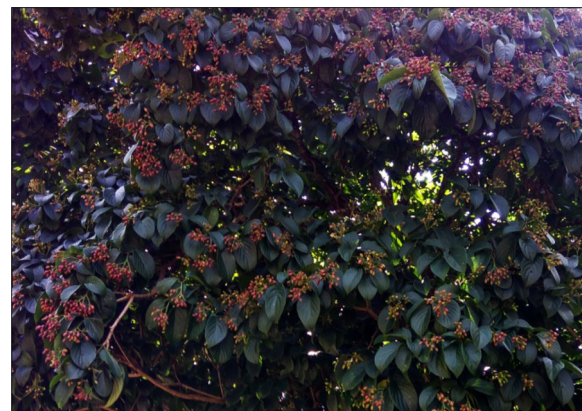


Fig. 1. Photograph for *N. nimmoniana* fruits.

man No. 1 filter paper twice. The resultant filtrate was stored at 4 °C and used as reducing and stabilizing agent.

2.3. Synthesis of silver nanoparticles

AgNPs was synthesized according to the method described by Roy et al. [29]. Briefly, the reaction mixture was prepared from 0.34 g of AgNO_3 which was dissolved in 100 mL of water. For preparing biogenic silver nanoparticles, 100 mL of fruit extract was added drop wise to 100 mL of silver nitrate solution (conc. 20 mM) so that the final concentration of the mixture remained 10 mM. The reaction mixture was kept at room temperature for 24 h in dark condition and color change pattern from yellow to dark brown indicates the formation of AgNPs.

2.4. Characterization techniques of silver nanoparticles

2.4.1. Ultraviolet-visible (UV-vis) spectra

The initial characterization of silver ion reduction to AgNPs was monitored by Shimadzu 1700 UV-vis spectrophotometer with a resolution of 1 nm the between the wavelength range of 200 and 700 nm. Distilled water was utilized as the blank.

2.4.2. FT-IR spectroscopy analysis

The Fourier Transform Infrared (FT-IR) spectra were recorded with an FT-IR spectrophotometer (Shimadzu, 8400, Japan) using KBr. The powdered sample was mixed with KBr. The scans recorded were the average of 100 scans and the selected spectral range between 400 and 4000 cm^{-1} .

2.4.3. Powder X-ray diffraction (XRD)

The red solid product was separated by repeated centrifugation at 12,000 rpm for 10 min followed by redispersion of the pellet of SNPs into deionized water three times. The solid was then dried in an oven at 60 °C. The X-ray diffraction (XRD) pattern was obtained with a PW 1800 Philips diffractometer using $\text{Cu-K}\alpha$ radiation ($\lambda = 0.1541 \text{ nm}$), and the data were collected from 20° to 80° (2θ) with a scan speed of 4 min^{-1} .

2.4.4. Scanning Electron Microscopy (SEM) and energy dispersive X-ray (EDX) analysis

Scanning electron microscopic (SEM) analysis was performed using the SIGMA model, CASL ZEISS, German operated at an accelerating voltage of 10 kV. The sample was prepared on a carbon coated copper grid by simply dropping a very small amount of the sample on the grid and using blotting paper excess solution were removed. The film was then allowed to dry under a mercury lamp for 5 min. For EDX analysis, the AgNPs were dried and drop coated on to carbon film. EDX analysis was then performed using the Oxford instrument Thermo EDX attached with SEM.

2.4.5. Particle size and zeta potential analysis

The aqueous suspension of the synthesized nanoparticles was filtered through a 0.22 µm syringe driven filter unit, and the size and distribution of the nanoparticles were measured using dynamic light scattering technique by ZETA Seizers Nanoseries (Malvern Instruments Nano ZS).

2.5. Determination of total phenolics, flavonoid and tannin contents

The total phenolic content was determined according to the method described by Siddhuraju and Becker [30]. The results were expressed as Gallic acid equivalents. The tannins were estimated after the extracts treated with polyvinyl polypyrrolidone (PVPP) [31]. The tannin content of the sample was calculated as follows: Tannins = Total phenolics – Non tannin phenolics. The flavonoid contents of the extracts were measured according to the method described by Zhishen et al. [32]. All the experiments were done in triplicate and the results expressed in rutin equivalents.

2.6. Antioxidant activity

2.6.1. 1,1-Diphenyl-2-picrylhydrazyl radical scavenging activity

The antioxidant activity of the extract was determined in terms of hydrogen donating or radical scavenging ability using the stable radical 1,1-diphenyl-2-picrylhydrazyl (DPPH), according to the method of Blois [33]. The results were expressed as IC₅₀ which is the concentration of the sample required to inhibit 50% of DPPH concentration.

2.6.2. 2,2'-Azino-bis(3-ethylbenzothiazoline-6-sulfonic acid)⁺• scavenging activity

The total antioxidant activity of the samples was measured by 2,2'-azino-bis(3-ethylbenzothiazoline-6-sulphonic acid) (ABTS)⁺• decolorization assay according to the method of Re et al. [34]. The unit of total antioxidant activity (TAA) is defined as the concentration of trolox having an equivalent antioxidant activity and expressed as mM trolox equivalents/g sample extract.

2.6.3. Ferric reducing antioxidant power assay

The antioxidant capacities of different extract of samples were estimated according to the procedure described by Pulido et al. [35]. Equivalent concentration was estimated as the concentration of antioxidant giving an absorbance increase in the ferric reducing antioxidant power (FRAP) assay equivalent to the theoretical absorbance value of a 1 mmol/L concentration of Fe(II) solution. Equivalent concentration was estimated as the concentration of antioxidant giving an absorbance increase in the FRAP assay, which is tantamount to the theoretical absorbance value of a 1 mmol/L concentration of Fe(II) solution.

2.6.4. Phosphomolybdenum assay

The antioxidant activity of samples was evaluated by the green phosphomolybdenum complex formation according to the method of Prieto et al. [36]. The results reported are mean values expressed as mg of ascorbic acid equivalents/g extract.

2.6.5. Metal chelating activity

The chelating activities of samples and standards were estimated using the method of Dinis et al. [37]. An aliquot of 0.1 mL AgNPs and fruit extract, 0.6 mL distilled water and 0.1 mL ferrous chloride (2 mmol/L) was well mixed and incubated for 30s. Then, 0.2 mL ferrozine (5 mmol/L) was added to the above mixture and incubated for 10 min at room temperature and the absorbance was recorded at 562 nm with UV-vis spectrophotometer. EDTA (0–2 µg) was used as a standard for the preparation of calibration curve. The metal chelating ability of antioxidant was expressed as mg EDTA/g.

2.7. Antibacterial activity

2.7.1. Disc diffusion method

The antibacterial potential of biofunctionalized AgNPs and fruit extract were tested against *Bacillus subtilis* (MTCC-441), *Escherichia coli* (MTCC-724), *Staphylococcus aureus* (MTCC96), *Salmonella paratyphi* (MTCC-735), *Proteus vulgaris* (MTCC-426), *Aeromonas hydrophila* (MTCC-7646) and *Klebsiella pneumoniae* (MTCC-432) bacteria by using agar disc diffusion according to standard methods (NCCLS 2000). About 20 mL of molten and cooled nutrient agar media was poured into sterilized Petri dishes. The plates were left overnight at room temperature to allow any contamination to appear. The discs were placed on Muller Hinton agar plates inoculated with each of the previously mentioned microorganisms and 20 µg/mL of Ag-NPs and fruit extracts were placed on inoculated agars. The test plates were incubated at 37 °C for 24 h. Later on the incubation period, the zone of inhibition (in millimeter diameter) was noted and tabulated. Streptomycin was used as an antibacterial standard against all pathogens. Experiments were performed in triplicate.

2.7.2. Minimum inhibitory concentration of silver nanoparticles

The minimum inhibitory concentration (MIC) of silver nanoparticles was determined according (Clinical Laboratory Standards Institute (CLSI)) to the standard broth micro-dilution

method [38]. Two-fold serial dilutions of known concentrations of AgNPs extract (800, 400, 200, 100, 50, 25, 12.5, 6.25, 3.12, 1.5, 0.78, 0.39 and 0.19 µg/mL) and antibiotic was made using Mueller–Hinton broth with appropriate control. To each well, 100 µL inoculum ($\approx 5 \times 10^5$ CFU/mL) was added and were incubated at 37 °C for 20 h. The lowest concentration which completely inhibited the growth of microbes was recorded as MIC. From the above assay, a loopful of inoculums was taken from each well showing no visual growth after incubation and spotted onto Mueller–Hinton plates to validate the MIC assay. All the experiments were performed in triplicate.

2.8. Cytotoxicity assay

The cytotoxicity studies of fruit extract capped AgNPs and the crude fruit extract were performed on HeLa cell lines using 3-(4,5-dimethylthiazol-2-yl)-2,5-diphenyltetrazolium bromide (MTT) assay. The cells were seeded in 96-well tissue culture plates at a 1.5×10^4 cells/well allowed to attach for 24 h and treated with different concentrations (6.25, 12.50, 25, 50 and 100 µg/mL) of AgNPs. After 24 h of incubation (37 °C in 5% CO₂ humid atmosphere) 100 µL (5 mg/mL) of MTT was added to each well and incubated for 4 h at 37 °C under 5% CO₂ humid atmosphere until a purple precipitate was visible. Media was removed carefully (do not disturb cells and do not rinse with PBS). 150 µL of DMSO (MTT solvent) was added to dissolve the purple precipitate. The absorbance was read at 570 nm with microplate spectrophotometer (Bio-Rad, Richmond, CA), using wells containing cells without sample as controls. Measurements were performed in triplicates, and the concentration required for 50% inhibition of viability (IC₅₀) was determined graphically. The effect of the samples was expressed as the % cell viability, using the following formula:

$$\% \text{Cell viability} = \frac{\text{Absorbance at } 570 \text{ nm of treated cells}}{\text{Absorbance at } 570 \text{ nm of control cells}} \times 100$$

3. Results and discussion

3.1. Characterization of synthesized AgNPs from fruit extract of *N. nimmoniana*

In the present study, synthesis of AgNPs was performed using fruit extract of *N. nimmoniana* and their biological activities were also assessed under *in vitro* condition. The advancement of green syntheses over chemical and physical methods is: environment friendly, cost effective and easily scaled up for large scale syntheses of nanoparticles, furthermore there is no need to use high temperature, pressure, energy and toxic chemicals [39]. A lot of literature has been reported to till date on biological syntheses of silver nanoparticles using microorganisms including bacteria, fungi and plants; because of their antioxidant or reducing properties typically responsible for the reduction of metal compounds in their respective nanoparticles. Although; among various biological methods of silver nanoparticle syn-



Fig. 2. Photograph showing the color change pattern during nanoparticle synthesis; (A) crude fruit extract of *N. nimmoniana* (50 mg/mL); (B) AgNO₃ with the fruit extract forming AgNPs after 1 h of incubation.

thesis, microbe mediated synthesis is not of industrial feasibility due to the requirements of highly aseptic conditions and their maintenance. Therefore; the use of plant extracts for this purpose is potentially advantageous over microorganisms due to the ease of improvement, the less biohazard and elaborate process of maintaining cell cultures [40]. It is the best platform for syntheses of nanoparticles; being free from toxic chemicals as well as providing natural capping agents for the stabilization of silver nanoparticles [41].

The characterization of nanoparticles is usually done based on their shape, size, surface area and dispersion. Plant mediated synthesis of nanoparticles has nowadays become popular because these biosynthesized nanoparticles, which are uniform and stable in nature. Thus, it could be used for its ample applications in various fields [42,43]. However, nanoparticle size, shape and formation differ among different plant species because of the reaction with metal ions and various biomolecules in the plant extract [42]. In our study, the fruit extract of *N. nimmoniana* changed its color from yellow to dark brown when mixed with AgNO₃ at room temperature within 1 h of incubation (Fig. 2). The color change by metallic nanoparticles is due to the coherent excitation of all “free” electrons which are released by the phenolic compounds present in the fruit extracts. This is in agreement with the finding of the previous researchers who reported that the color change is an indication of the formation of AgNPs in various plant systems [24,26]. Ahmad et al. [44] explained the main reason behind the color change is the surface plasmon resonance of the metal nanoparticles. However, the reaction time and the intensity of color formed varied amongst the plants and species [16,21,28,29].

The reducing capacity depends on the amount of hydrolysable tannins, polyphenols and flavonoids present in the *Nothapodytes* extract. During the reaction with silver nitrate, the phenolic com-

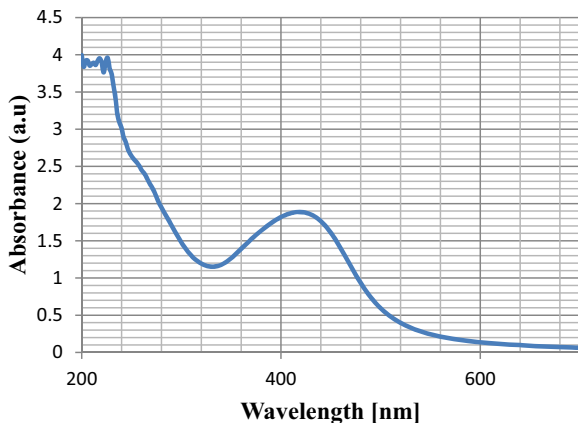


Fig. 3. UV-vis spectra of synthesized AgNPs using fruit extract of *N. nimmoniana*.

pound donates electron to Ag^+ to produce Ag^0 . After donation of an electron, the phenolic compounds changed into quinone which is stabilized by the resonance structure of the same. The bioreduction of silver ions and the formation of AgNPs are closely related to the biomolecular component of the extract. Biosynthesis is a green process, no by-products and wastage formed during the reaction [45]. In the present study indicates that the color change in the fruit extract within 1 h of incubation. However, the greatest intensity of color change was observed after 8 h of the reduction reaction with AgNO_3 . Presence of phytochemicals such as alkaloids, flavonoids, saponins, terpenoids, steroids and proteins in the fruit extract of *N. nimmoniana* appears to be responsible for accelerating the reduction reaction and capping of AgNPs synthesis.

3.1.1. UV-vis spectra of Ag nanoparticles

UV-vis spectroscopy analysis indicated a sharp plasmon resonance at around 416 nm, which was specific for AgNPs (Fig. 3). Similarly, several earlier researchers have also observed the absorption spectrum between 410 and 450 nm due to surface plasmon resonance in AgNPs [46,47].

3.1.2. FT-IR analysis

FT-IR spectroscopy measurements are carried out to identify the biomolecules that bound specifically to the silver surface and possible biomolecules responsible for the capping agent on the nanoparticles. The spectrum of *N. nimmoniana* fruit extract (Fig. 4A) and AgNPs (Fig. 4B) shows a shift in the following peaks $3406.64\text{--}3429.78$, $1612.2\text{--}1604.48$, $1383.68\text{--}1401.03$, $1061.62\text{--}1120.44$, $593.004\text{--}619.038\text{ cm}^{-1}$. The absorption peak at 3406.64 cm^{-1} observed in fruit extract, which is due to OH stretching vibration and shifted to higher frequency regions (3429.78 cm^{-1}). The band 1612.2 cm^{-1} was due to the presence of $\text{C}=\text{O}$ stretching and was shifted to lower frequency (1604.48 cm^{-1}) in AgNPs, when compared with the fruit extract. The band appearing at 1384 cm^{-1} in fruit extract was due to the presence of $\text{C}=\text{N}$ stretching of amine group and this was shifted to 1401.03 cm^{-1} in AgNPs because of the proteins that possibly will bind to AgNPs through the amine groups. On the other hand, the band shift at 1120.44 cm^{-1} was attributed to the

binding of the C–O functional group with silver nanoparticles. The peak at 593.004 and 619.038 cm^{-1} indicates C–Br bending of the alkyl halides groups. Furthermore, the result shows that the phytochemical constituents such as alkaloids, phenolic compounds, amino acids, carbohydrates and particularly tannins may protect the AgNPs from aggregation and thereby retain the long term stability of nanoparticles.

3.1.3. SEM along with EDX analysis

The AgNPs were observed predominately adopt a near spherical morphology with smooth surface under the Scanning Electron Microscopy in different magnifications micrometer (μm) to nanometer (nm). The SEM images of AgNPs were assembled onto the surface due to the interactions such as hydrogen bond and electrostatic interactions between the bioorganic capping molecules bound to the AgNPs [45]. A similar phenomenon has been reported previously, where the FE-SEM micrograph shows crystalline spherical AgNPs [48]. The sizes of the particles were ranging from 46 to 235 nm as shown in Fig. 5A. Fig. 5B shows the maximum size of the silver nanoparticles obtained was between 60–80 nm.

The information of elemental compositions for Ag NPs was carried by EDX analysis and is depicted in Fig. 5C. EDX spectrum confirmed the presence of strong elemental signal of the silver at 3 keV which is typical for the absorption of metallic silver nanocrystallites due to surface Plasmon resonance [49]. Apart from silver peaks, there are weaker signals from Ca, O and C atoms were also recorded. These weaker signals are likely to be due to X-ray emission from proteins/enzymes present in the *N. nimmoniana* fruit extract of the biomass. Ag ion peaks are present in two places because of the X-ray signal from AgNO_3 and leaf extract contain Ag related inorganic compounds.

3.1.4. Dynamic light scattering and zeta potential analysis

Dynamic light scattering (DLS) analysis determined the average particle size distribution profile of synthesized nanoparticles and capping agent enveloped the metallic particles along with the particular size of the metallic core [32]. In our result, the size of AgNPs is in the range $31.71\text{--}153.7\text{ nm}$ and Z-average size is 238.0 nm (Fig. 6A). In addition, some of the large sized particles appeared in DLS result which is due to the agglomeration AgNPs in the solution. Zeta potential (ZP) is an important parameter for understanding the state of the nanoparticle surface and predicting the long-term stability of the dispersion. According to previous reports, nanoparticles with zeta potential values greater than $+25\text{ mV}$ or less than -25 mV typically has high degrees of stability. In our work, the ZP value of the synthesized AgNPs is -23.1 mV (Fig. 6B).

3.1.5. XRD studies

The XRD pattern of the synthesized AgNPs from the fruit extract of *N. nimmoniana* showed the distinctive peaks indexed to the crystal planes of face centered cubic silver (Fig. 7). The diffraction profile had an intense peak at 2θ of 38.2442° , 44.4257° , 64.6076° , and 76.3839° , corresponds to (1 1 1), (2 0 0), (2 2 0), and (3 1 1) planes respectively. Our result is in conformity with the reports of the Joint Committee on Powder

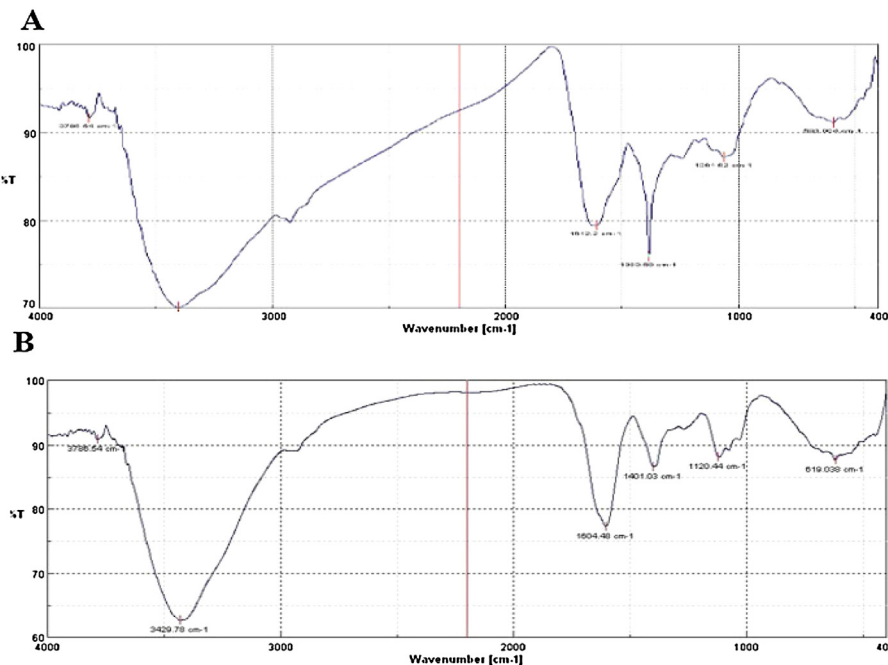


Fig. 4. FT-IR; (A) FT-IR spectra of crude fruit extract of *N. nimmoniana*; (B) FT-IR spectra of synthesized AgNPs displays the interaction of nanoparticles with plant biocompound.

Diffraction Standards (JCPDS No. 89-3722). The peaks were very sharp and clearly indicated that the AgNPs are synthesized under nano-regime have crystalline nature. Similar observations were also recorded by earlier researchers [49–52]. The average grain size of the Ag NPs was determined using Scherers equation,

$$D = \frac{k\lambda}{\beta \cos\theta}$$

where k is the shape factor (0.94), d is the mean diameter of the nanoparticle, λ is the wavelength of the X-ray, β is the angular width at FWHM of the X-ray diffraction peak at Bragg's diffraction angle θ . The average size of the Ag NPs is estimated to be around 69 nm using Scherer's equation.

3.2. Total phenolics, tannins and flavonoid contents

The effects of total phenolics, tannins and flavonoid content of *N. nimmoniana* fruit extracts are shown in Table 1. The fruit extract recorded the highest total phenolic content (194.56 ± 3.15 mg GAE/g extract) compared to AgNPs. In addition to it, the fruit extract also recorded the maximum content of tannin (48.20 ± 2.03 mg GAE/g extract) and flavonoid (283.33 ± 7.18 mg RE/g extract). Phenolic and flavonoids have been reported to be the most important phytochemicals responsible for the antioxidant capacity. Plant-derived polyphenols display characteristic inhibition patterns toward the oxidative response. Thus, the higher amount of phenolics, tannins and flavonoid contents in fruit extract of *N. nimmoniana* can be taken as a fine indication of its higher antioxidant capability. On comparing with the earlier report in *Syzygium cumini* recorded higher

total phenolics and flavonoids contents in plant extract than the AgNPs [53].

3.3. Antioxidant activity

The free radical scavenging activity of synthesized AgNPs and fruit extract were determined by using different *in vitro* assays. DPPH[•] radical has been widely used to test the ability of compounds to act as free radical scavengers or hydrogen donors and thus to evaluate the antioxidant activity [53]. The lower value of IC₅₀ indicates a higher antioxidant activity. In DPPH[•] radical scavenging, the highest activity (Fig. 8) was observed in fruit extracts of *N. nimmoniana* ($3.88 \mu\text{g/mL}$). This value was significantly higher over positive standards. Substantial DPPH radical scavenging capacity of the fruit extract could be explained by the presence of phenolic components [53]. The presence of tannins and flavonoids in *Nothapodytes* fruit extract also contributed to high DPPH radical scavenging activity of this extract. Further, alkaloids are usually the major component identified in the fruit and expected to contribute hydrogen donating ability. Similar observation has been reported in *Piper longum* [54], *Iresine herbstii* [55], *Chenopodium murale* [56], *Morinda pubescens* [57], *Nelumbo nucifera* [58] and *Areca catechu* [59] silver nanoparticles.

In FRAP assay, the ability of *N. nimmoniana* extracts to reduce Fe³⁺ to Fe²⁺ ranges from 2114.89 ± 267.54 to 4136.09 ± 437.31 mmol Fe(II)/g extract (Table 2). All the extracts exhibited significant reducing ability higher than that of positive control BHT (3582.39 ± 114.39). This might be due to the presence high phenolic concentration in the fruit extract. Similar observations were made by Dipankar and Murugan [55]

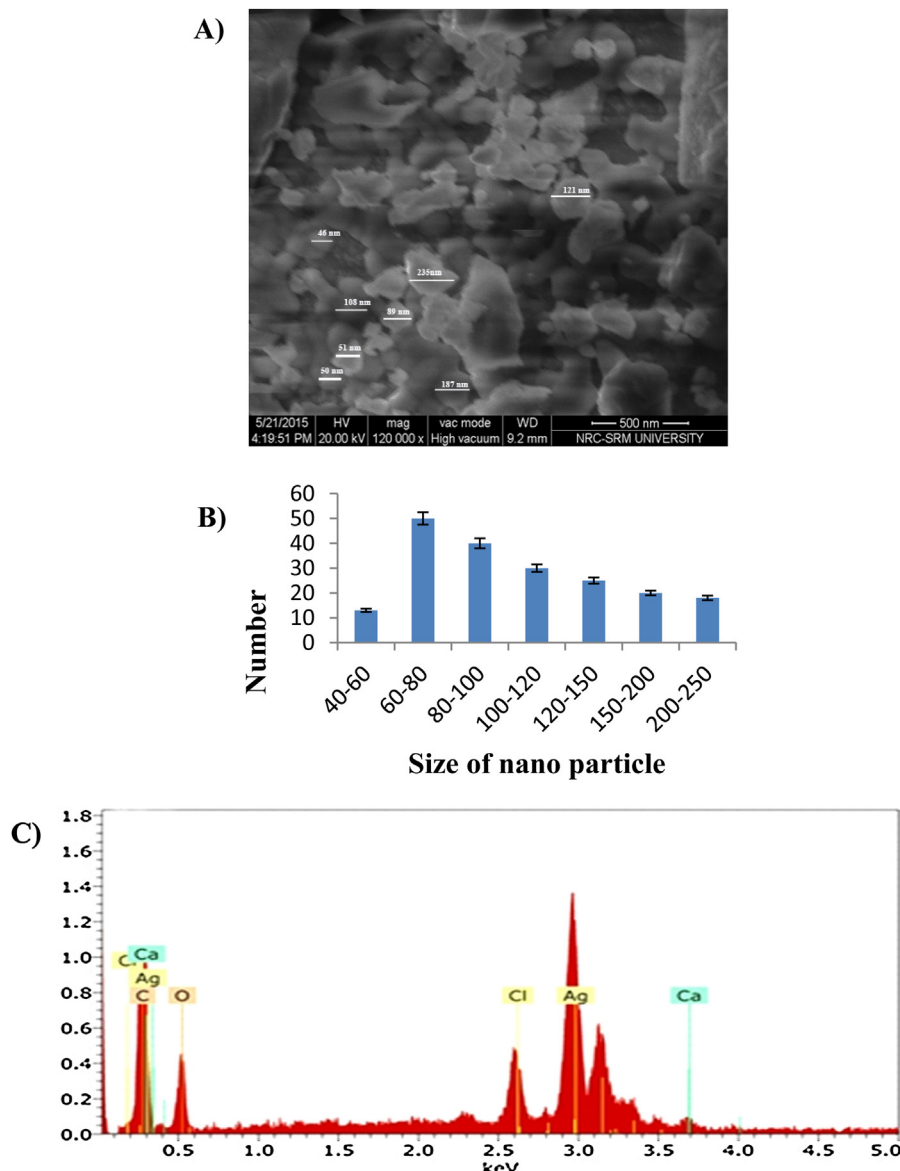


Fig. 5. SEM images of synthesized AgNPs using fruit extract of *N. nimmoniana*. (A) SEM image of synthesized AgNPs in colloidal condition at different nanometric scales. (B) Particle size of the synthesized AgNPs using fruit extract of *N. nimmoniana*. (C) EDAX images showing the presence of silver nanoparticles and bioorganic components *N. nimmoniana*.

Table 1

Total phenolics, tannin and flavonoid contents of synthesized AgNPs and crude fruit extract of *N. nimmoniana*.

Samples	Total phenolics (mg GAE/g extract)	Tannin (mg GAE/g extract)	Flavonoids (mg RE/g extract)
AgNPs	89.09 ± 4.97	17.10 ± 2.19	161.26 ± 2.02
Fruit extract	194.56 ± 3.15	48.20 ± 2.03*	283.33 ± 7.18*

Values are means of three independent analyses ± standard deviation (n=3). Mean values followed by different superscript letters indicate significant statistical difference ($p < 0.05$).

and Reddy et al. [54] in *I. herbstii* and *P. longum* silver nanoparticles.

ABTS⁺ radicals are more reactive than DPPH radicals; unlike the reactions with DPPH radicals, which involve H-atom transfer, the reactions with ABTS⁺ radicals involve an electron transfer process. As is seen in Table 2. The fruit extract of

N. nimmoniana registered the highest radical cation scavenging activity ($2592.24 \pm 135.67 \mu\text{mol/L}$ trolox equivalent/g extract). This might be due to the presence of higher levels of phenolic compounds, including tannins and flavonoids in fruit extract.

The phosphomolybdenum assay is successfully used to determine the ability of extracts to reduce Mo(VI) to Mo(V) and

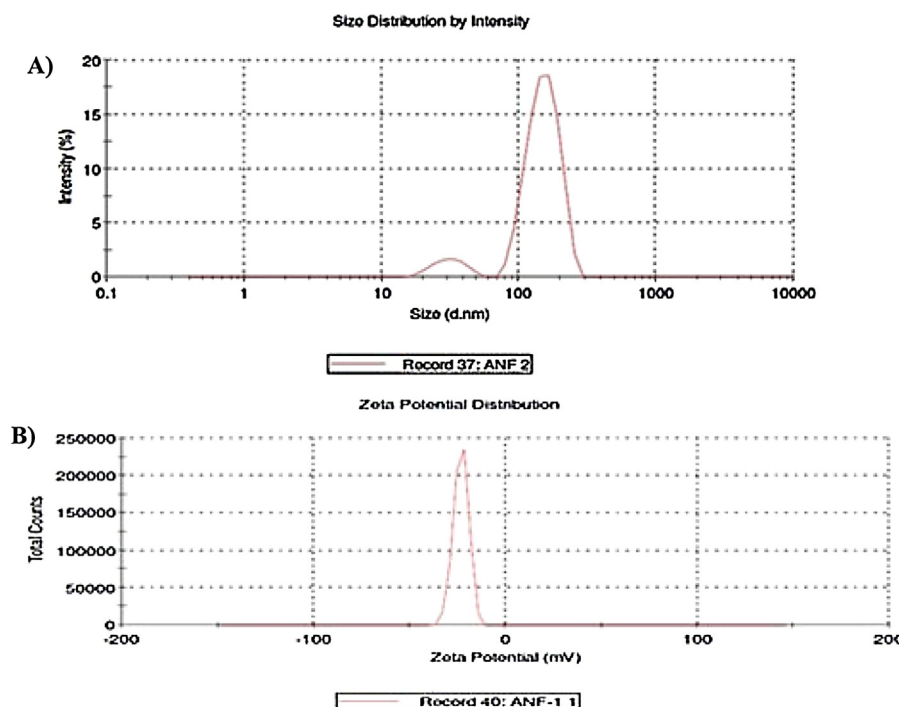


Fig. 6. (A) Size distribution of AgNPs measured by the DLS technique. (B) Zeta potential of the synthesized AgNPs using fruit extract of *N. nimmoniana*.

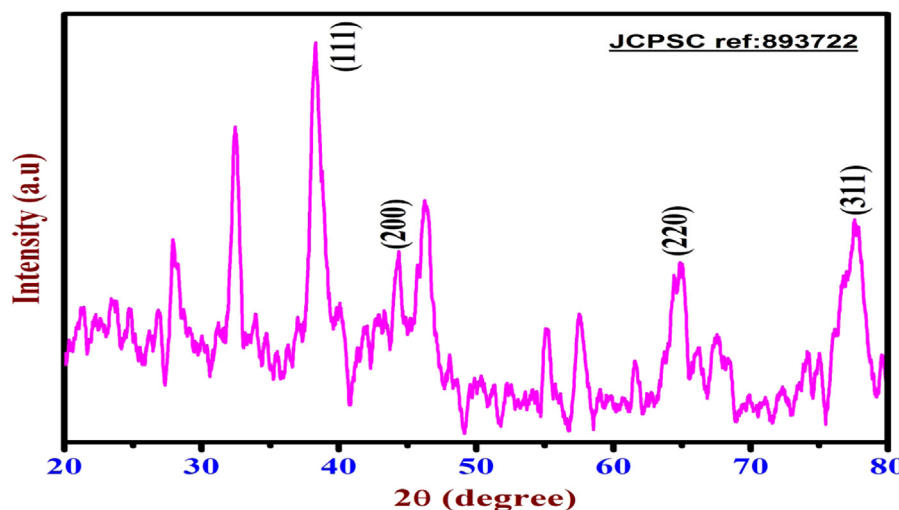


Fig. 7. X-ray diffraction patterns of synthesized AgNPs using fruit extract of *N. nimmoniana*.

Table 2

ABTS^{•+}, FRAP, metal chelating and phosphomolybdenum activities of synthesized AgNPs and crude fruit extract of *N. nimmoniana*.

Samples	FRAP (mmol Fe(II)/mg extract)	ABTS ^{•+} (μ mol/L trolox equivalents/g extract)	Metal chelating activity (mg EDTA/g extract)	Phosphomolybdenum (mg ascorbic acid equivalents/g)
AgNPs	2114.89 ± 267.54	1494.81 ± 245.55	98.41 ± 20.49	368.88 ± 4.08
Fruit extract	4136.09 ± 437.31*	2592.24 ± 135.67*	167.98 ± 23.76	491.41 ± 10.09*
BHT	3582.39 ± 114.39	22697.4 ± 350.81	–	489.39 ± 13.26

Values are means of three independent analyses ± standard deviation (n=3). Mean values followed by different superscript letters indicate significant statistical difference (p<0.05).

subsequent formation of green phosphate/Mo(V) complex at an acid pH. The results were expressed as mg ascorbic acid equivalents/g. The fruit extract exhibited powerful antioxidant

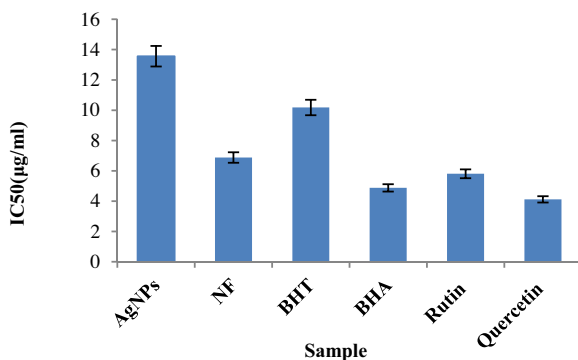
activity of 491.41 ± 10.09 mg ascorbic acid equivalents/g compared to that of the standard BHT 489.39 ± 13.26 mg ascorbic

Table 3

Antibacterial activity of synthesized AgNPs and fruit extract of *N. nimmoniana* against the human pathogenic bacterial strains.

Culture	Zone of inhibition (mm ± SE)		
	Standard	Fruit extract	AgNPs
<i>Bacillus subtilis</i> (MTCC-441)	13.00 ± 0.90	10.66 ± 0.44	10.66 ± 1.20
<i>Escherichia coli</i> (MTCC-724)	10.10 ± 1.27	10.02 ± 1.18	21.0 ± 2.14
<i>Staphylococcus aureus</i> (MTCC-96)	13.33 ± 1.52	9.00 ± 1.23	11.55 ± 0.03
<i>Salmonella paratyphi</i> (MTCC-735)	13.00 ± 1.00	13.00 ± 1.00	16.00 ± 1.07
<i>Proteus vulgaris</i> (MTCC-426)	12.45 ± 0.93	9.60 ± 0.91	15.00 ± 1.29
<i>Aeromonas hydrophila</i> (MTCC-7646)	10.70 ± 0.26	8.30 ± 0.21	11.33 ± 0.09
<i>Klebsiella pneumoniae</i> (MTCC-432)	10.66 ± 1.42	12.50 ± 0.52	24.00 ± 0.12

Streptomycin (20 µg/mL) was used as a positive control. Each value represents the mean ± standard error of three replicates per treatment.

Fig. 8. Antioxidant activity (DPPH free radical scavenging assay) of fruit extracts and synthesized AgNPs of *N. nimmoniana*.

acid equivalents/g (Table 2). Similar result was also observed in *M. pubescens* synthesized silver nanoparticles [54].

The metal ion chelating activity of the extracts was analyzed and shown in Table 2. The decolorization of the red color of the reaction mixture depends upon the reduction of ferrous ions by the plant extracts. The results were expressed as mg EDTA equivalents/g. Among the two extracts, the fruit extract showed higher activity (167.98 ± 23.76 mg EDTA/g extract).

3.4. Antimicrobial activity

It is evident from our study that the synthesized AgNPs and fruit extract had antimicrobial activity against all the tested human pathogens are shown in Table 3. The synthesized AgNPs were found to have higher inhibitory action when compared to the fruit extract. Moreover, AgNPs exhibit effective zone of inhibition against gram-negative bacteria (*S. paratyphi*, *E. coli* and *K. pneumoniae*) compared to the gram-positive bacteria (*S. aureus* and *B. subtilis*, *P. vulgaris* *A. hydrophila*). Among the various tested bacterial strains *K. pneumoniae* and *E. coli* were the most susceptible towards the AgNPs. The highest zone of inhibition (24.00 ± 0.12 mm) was recorded by *K. pneumoniae* and least zone of inhibition was recorded with (10.66 ± 1.20) *B. subtilis*. Antibacterial effects of AgNPs obeyed an action mechanism of antibacterial activity. The potential reason for the antibacterial activity of silver is that AgNPs may attach to the surface of the cell membrane disturbing permeability and respiration functions of the cell. Smaller AgNPs having the large surface area available for interaction would give more antibacte-

rial effect than the larger AgNPs. It is also possible that AgNPs not only interact with the surface of the membrane, but can also penetrate inside the bacteria.

3.4.1. Minimum inhibitory concentration of silver nanoparticles

MIC was recorded as the lowest concentration at which no visible growth of test pathogens was observed. Silver nanoparticles synthesized from *N. nimmoniana* showed appreciable antimicrobial activity against *E. coli* *K. pneumoniae* and *S. paratyphi* is exhibiting MIC of $3.12 \mu\text{g}/\text{mL}$. Similarly, $6.25 \mu\text{g}/\text{mL}$ was found to be MIC for, *S. aureus*, *P. vulgaris* and *B. subtilis* while $12.50 \mu\text{g}/\text{mL}$ was proved as MIC against *A. hydrophila*. In addition, the obtained results were validated using Mueller–Hinton plates which showed no organisms in it. On the other hand, Devi and Joshi [60] have observed $15 \mu\text{mol}/\text{L}$ and $20 \mu\text{mol}/\text{L}$ as MIC for Gram-negative and Gram-positive bacteria, respectively. In this work, the fruit based synthesized silver nanoparticles displayed significantly higher antimicrobial activity against Gram-negative bacteria than the Gram-positive singles. This is more likely due to the difference in the cell wall composition between these two groups.

3.5. Anticancer activity of synthesized AgNPs

In vitro cytotoxicity of the AgNPs was evaluated against HeLa cells at different concentrations. When the plant extract alone was tested for anticancer activity, we found that the viability of cancer cells decreased with an increase in the concentration of extract from 6.25 to $200 \mu\text{g}/\text{mL}$ (Fig. 9a) showing the potency of the extract alone in inhibiting cancer cells. Interestingly, when we experienced the efficacy of synthesized AgNPs against HeLa, we establish a staged decrease in cell viability when the concentration of the biologically synthesized AgNPs was increased (6.25 – $100 \mu\text{g}/\text{mL}$, Fig. 9b) and there was a dose dependent reduction in cell viability. It be supposed to be well-known that the concentration of synthesized AgNPs used in this case was very less when compared to extract. This diminish in cell viability with increase in AgNPs concentration, suggests that more number of AgNPs could accumulate inside cells, resulting in improved stress, finally leading to cell death (Fig. 9C). These results clearly exhibit the improved strength of AgNPs against cancer cells. These results also guide us

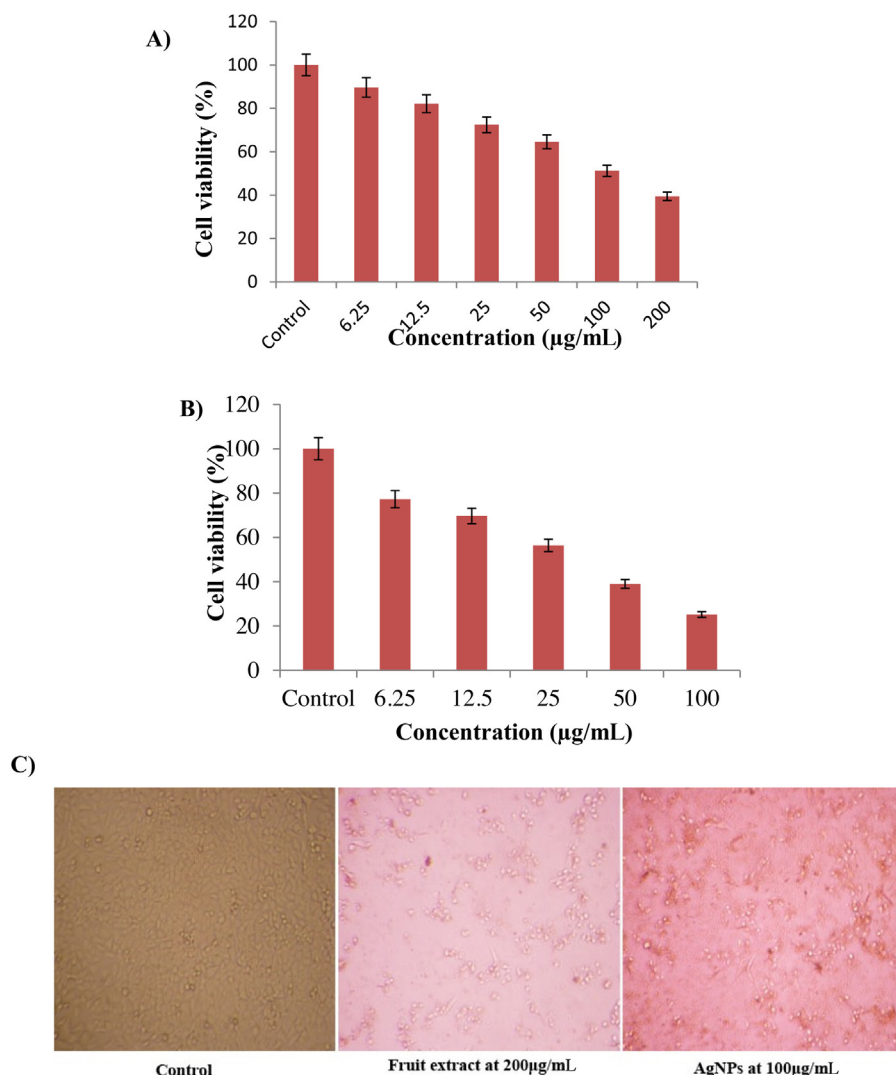


Fig. 9. Cytotoxicity assay of synthesized AgNPs and fruit extracts of *N. nimmoniana*. (A) Cytotoxicity of crude fruit extract on HeLa cells: All the data were expressed in mean \pm SD of three experiments. (B) Synthesized AgNPs treated HeLa cell line. All the data were expressed in mean \pm SD of three experiments. (C) HeLa cell growth of control, fruit extract and AgNPs.

to guess that with the increase in efficacy of AgNPs against cancer cells, the dosage could be effectively reduced without compromising the drug efficiency [61]. A few *in vitro* studies have previously shown translocation of AgNPs in cancer cell line with an IC₅₀ value of 300 µg/mL. In the present study, IC₅₀ values of AgNPs was 87.32 ± 1.43 µg/mL when compared to fruit extract showed 161.02 ± 3.92 µg/mL. In fact, inside cancer cells AgNPs may induce reactive oxygen species and cause damage to cellular components leading to cell death [62].

4. Conclusion

Silver nanoparticles are produced by the reduction of silver ions to colloidal silver. The present studies were confirmed the formation of silver nanoparticles using *N. nimmoniana* fruit extract from UV-vis, XRD, FE-SEM, and with EDX and FTIR respectively. In addition, antibacterial and cytotoxicity assessment of biosynthesized AgNPs shows enhanced antimicrobial

and anticancer potential. The findings of our study, suggest that synthesized AgNPs can be developed into a promising drug candidate for biomedical applications.

Acknowledgment

Author G. Mahendran thankful to University Grants Commission (UGC), New Delhi, India for providing financial assistance in the form of Dr. D. S. Kothari Postdoctoral Fellowship (BSR/BL/14-15/0100).

References

- [1] J.M. Gutteridge, Free radicals in disease processes: a compilation of cause and consequence, *Free Radic. Res. Commun.* 19 (1993) 141–158.
- [2] B. Halliwell, J.M. Gutteridge, Role of free radicals and catalytic metal ions in human disease: an overview, *Methods Enzymol.* 186 (1990) 1–85.
- [3] T. Finkel, N.J. Holbrook, Oxidants, oxidative stress and the biology of ageing, *Nature* 408 (2000) 239–247.

- [4] V. Lobo, A. Patil, A. Phatak, N. Chandra, Free radicals, antioxidants and functional foods: impact on human health, *Pharmacogn. Rev.* 4 (8) (2010) 118–126.
- [5] V.V. Mody, R. Siwale, A. Singh, R.H. Mody, Introduction to metallic nanoparticles, *J. Pharm. Bioallied Sci.* 2 (2010) 282–289.
- [6] K. Shameli, M.B. Ahmad, W.Z.W. Yunus, N.A. Ibrahim, M. Darroudi, Synthesis and characterization of silver/talc nanocomposites using the wet chemical reduction, *Int. J. Nanomed.* 5 (2010) 743–751.
- [7] B. Yin, H. Ma, S. Wang, S. Chen, Electrochemical synthesis of silver nanoparticles under protection of poly(*N*-vinylpyrrolidone), *J. Phys. Chem. B* 107 (2003) 8898–8904.
- [8] M. Darroudi, M.B. Ahmad, M. Hakimi, R. Zamiri, A. Khorsand Zak, H.A. Hosseini, M. Zargar, Preparation, characterization and antibacterial activity of γ -irradiated silver nanoparticles in aqueous gelatin, *Int. J. Miner. Metall. Mater.* 20 (2013) 403–409.
- [9] M. Darroudi, M.B. Ahmad, A.K. Zak, R. Zamiri, M. Hakimi, Fabrication and characterization of gelatin stabilized silver nanoparticles under UV-light, *Int. J. Mol. Sci.* 12 (2011) 6346–6356.
- [10] A.S. Kutsenko, V.M. Granchak, Photochemical synthesis of silver nanoparticles in polyvinyl alcohol matrices, *Theor. Exp. Chem.* 45 (2009) 313–318.
- [11] M. Darroudi, A. Khorsand Zak, M.R. Muhamad, N.M. Huang, M. Hakimi, Green synthesis of colloidal silver nanoparticles by sonochemical method, *Mater. Lett.* 66 (2012) 117–120.
- [12] G.A. Kahrlas, L.M. Wally, S.J. Fredrick, M. Hiskey, A.L. Prieto, J.E. Owens, Investigation of antibacterial activity by silver nanoparticles prepared by microwave-assisted green syntheses with soluble starch, dextrose and arabinose, *ACS Sustain. Chem. Eng.* 2 (2014) 367–376.
- [13] M. Darroudi, M.B. Ahmad, R. Zamiri, A.H. Abdullah, N.A. Ibrahim, A.R. Sadrolhosseini, Time-dependent preparation of gelatin-stabilized silver nanoparticles by pulsed Nd: YAG laser, *Solid State Sci.* 13 (2011) 520–524.
- [14] M. Darroudi, M.B. Ahmad, R. Zamiri, A.H. Abdullah, N.A. Ibrahim, K. Shameli, M.S. Husin, Preparation and characterization of gelatin mediated silver nanoparticles by laser ablation, *J. Alloys Compd.* 509 (2011) 1301–1304.
- [15] Q.H. Tran, V.Q. Nguyen, A.T. Le, Silver nanoparticles: synthesis, properties, toxicology, applications and perspectives, *Adv. Nat. Sci. Nanosci. Nanotechnol.* 4 (2013) 1–20.
- [16] C. Rajkuberan, K. Sudha, G. Sathishkumar, S. Sivaramakrishnan, Antibacterial and cytotoxic potential of silver nanoparticles synthesized using latex of *Calotropis gigantea* L, *Spectrochim. Acta A: Mol. Biomol. Spectrosc.* 136 (2015) 924–930.
- [17] T.J.I. Edison, M.G. Sethuraman, Instant green synthesis of silver nanoparticles using *Terminalia chebula* fruit extract and evaluation of their catalytic activity on reduction of methylene blue, *Process Biochem.* 47 (2012) 1351–1357.
- [18] A. Bankar, B. Joshi, A.R. Kumar, S. Zinjarde, Banana peel extract mediated novel route for the synthesis of silver nanoparticles, *Colloids Surf. A* 368 (2010) 58–63.
- [19] S. Singh, J.P. Saikia, A.K. Buragohain, A novel reusable PAni-PVA-Amylase film: activity and analysis, *Colloids Surf. B: Biointerfaces* 102 (2013) 83–85.
- [20] M. Umadevi, M.R. Bindhu, V. Sathe, A novel synthesis of malic acid capped silver nanoparticles using *Solanum lycopersicum* fruit extract, *J. Mater. Sci. Technol.* 29 (4) (2013) 317–322.
- [21] P.S. Ramesh, T. Kokila, D. Geetha, Plant mediated green synthesis and antibacterial activity of silver nanoparticles using *Emblica officinalis* fruit extract, *Spectrochim. Acta A: Mol. Biomol. Spectrosc.* 142 (2015) 339–343.
- [22] D. Jain, H.K. Daima, S. Kachhwaha, S.L. Kothari, Green synthesis of silver nanoparticles using *Argemone mexicana* leaf extract and evaluation of their antimicrobial activities, *Dig. J. Nanomater. Biostruct.* 4 (4) (2009) 723–727.
- [23] M.G. Moghaddam, R.H. Dabanlou, Plant mediated green synthesis and antibacterial activity of silver nanoparticles using *Crataegus douglasii* fruit extract, *J. Ind. Eng. Chem.* 20 (2) (2014) 739–744.
- [24] R. Subashini, S. Sruthi, P. Sindhuja, S. Santhini, D. Gnana Prakash, Biosynthesis of silver nanoparticles using *Garcinia mangostana* fruit extract and their antibacterial, antioxidant activity, *Int. J. Curr. Microbiol. Appl. Sci.* 4 (1) (2015) 944–952.
- [25] M. Medhi, Eco-friendly synthesis of silver nanoparticles using fruit extract of *Averrhoa Carambola*, *Int. J. Innov. Sci. Eng. Technol.* 1 (4) (2014) 479–482.
- [26] B. Kumar, K. Smita, L. Cumbal, A. Debut, *Lantana camara* berry for the synthesis of silver nanoparticles, *Asian Pac. J. Trop. Biomed.* 5 (3) (2015) 192–195.
- [27] T. Isah, A. Mujib, *In vitro* propagation and camptothecin production in *Nothapodytes nimmoniana*, *Plant Cell Tissue Organ Cult.* 121 (2015) 1–10.
- [28] B. Sadeghi, F. Gholamhosseinpoor, A study on the stability and green synthesis of silver nanoparticles using *Ziziphora tenuior* (Zt) extract at room temperature, *Spectrochim. Acta A: Mol. Biomol. Spectrosc.* 134 (2015) 310–315.
- [29] K. Roy, C.K. Sarkar, C.K. Ghosh, Photocatalytic activity of biogenic silver nanoparticles synthesized using potato (*Solanum tuberosum*) infusion, *Spectrochim. Acta A: Mol. Biomol. Spectrosc.* 146 (2015) 286–291.
- [30] P. Siddharaju, K. Becker, Antioxidant properties of various solvent extracts of total phenolic constituents from three different agroclimatic origins of drumstick tree (*Moringa oleifera* Lam.) leaves, *J. Agric. Food Chem.* 51 (2003) 2144–2155.
- [31] P. Siddharaju, S. Manian, The antioxidant activity and free radical-scavenging capacity of dietary phenolic extracts from horse gram (*Macrotyloma uniflorum* (Lam.) Verdc.) seeds, *Food Chem.* 105 (2007) 950–958.
- [32] J. Zhishen, T. Mengcheng, W. Jianming, The determination of flavonoid contents in mulberry and their scavenging effects on superoxide radicals, *Food Chem.* 64 (1999) 555–559.
- [33] M.S. Blois, Antioxidant determinations by the use of a stable free radical, *Nature* 26 (1958) 1199–1200.
- [34] R. Re, N. Pellegrini, A. Proteggente, A. Pannala, M. Yang, C. Rice-Evans, Antioxidant activity applying an improved ABTS radical cation decolorization assay, *Free Radic. Biol. Med.* 26 (1999) 1231–1237.
- [35] R. Pulido, L. Bravo, F. Sauco-Calixto, Antioxidant activity of dietary polyphenols as determined by a modified ferric reducing/antioxidant power assay, *J. Agric. Food Chem.* 48 (2000) 3396–3402.
- [36] P. Prieto, M. Pineda, M. Aguilar, Spectrophotometric quantitation of antioxidant capacity through the formation of a phosphomolybdenum complex: specific application to the determination of vitamin E, *Anal. Biochem.* 269 (1999) 337–341.
- [37] T.C.P. Dinis, V.M.C. Madeira, L.M. Almeida, Action of phenolic derivatives (acetaminophen salicylate, and 5-aminosalicylate) as inhibitors of membrane lipid peroxidation and as peroxyl radical scavengers, *Arch. Biochem. Biophys.* 315 (1994) 161–169.
- [38] J.M. Andrews, Determination of minimum inhibitory concentrations, *J. Antimicrob. Chemother.* 48 (2001) 5–16.
- [39] S. Dhuper, D. Panda, P.L. Nayak, Green synthesis and characterization of zero valent iron nanoparticles from the leaf extract of *Mangifera indica*, *Nano Trends: J. Nanotechnol. Appl.* 13 (2) (2012) 16–22.
- [40] K. Kalishwaralal, V. Deepak, R.K. Pandian, S.M. Kottaisamy Barathmani, K.S. Kartikeyan, B.S. Gurunathan, Biosynthesis of silver and gold nanoparticles using *Brevibacterium casei*, *Colloids Surf. B: Biointerfaces* 77 (2010) 257–262.
- [41] S. Ahmed, M. Ahmad, B.L. Swami, S. Ikram, A review on plants extract mediated synthesis of silver nanoparticles for antimicrobial applications: a green expertise, *J. Adv. Res.* 7 (2016) 17–28.
- [42] S. Ashokkumar, S. Ravi, V. Kathiravan, S. Velmurugan, Synthesis of silver nanoparticles using *A. indicum* leaf extract and their antibacterial activity, *Spectrochim. Acta A: Mol. Biomol. Spectrosc.* 134 (2015) 34–39.
- [43] M.K. Swamy, M.S. Akhtar, S.K. Mohanty, U.R. Sinniah, Synthesis and characterization of silver nanoparticles using fruit extract of *Momordica cymbalaria* and assessment of their in vitro antimicrobial, antioxidant and cytotoxicity activities, *Spectrochim. Acta A: Mol. Biomol. Spectrosc.* 151 (2015) 939–944.
- [44] N. Ahmad, S. Sharma, M.K. Alam, V.N. Singh, S.F. Shamsi, B.R. Mehta, Rapid synthesis of silver nanoparticles using dried medicinal plant of basil, *Colloid Surf. B* 81 (2010) 81–86.

- [45] R. Subramanian, P. Subbramaniyan, V. Raj, Antioxidant activity of the stem bark of *Shorea roxburghii* and its silver reducing power, Springer Plus 2 (28) (2013) 1–11.
- [46] J.J. Mock, M. Barbic, D.R. Smith, D.A. Schultz, S. Schultz, Shape effects in plasmon resonance of individual colloidal silver nanoparticles, J. Chem. Phys. 116 (2002) 6755–6759.
- [47] M. Rivallan, B.S. Thomas, M. Lepage, N. Takagi, H. Hirata, F.T. Starzyk, Evolution of platinum particles dispersed on zeolite upon oxidation catalysis and ageing, ChemCatChem 2 (2010) 1599–1605.
- [48] M.M. Priya, B.K. Selvi, J.A. John Paul, Green synthesis of silver nanoparticles from the leaf extracts of *Euphorbia hirta* and *Nerium indicum*, Dig. J. Nanomat. Biostruct. 6 (2011) 535–542.
- [49] K. Kalimuthu, R.S. Babu, D. Venkataraman, M. Bilal, S. Gurunathan, Biosynthesis of silver nanocrystals by *Bacillus licheniformis*, Colloids Surf. B 65 (2008) 150–153.
- [50] V. Kathiravan, S. Ravi, S. Ashokkumar, S. Velmurugan, K. Elumalai, C.P. Khatiwada, Green synthesis of silver nanoparticles using *Croton sparsiflorus* morong leaf extract and their antibacterial and antifungal activities, Spectrochim. Acta A: Mol. Biomol. Spectrosc. 139 (2015) 200–205.
- [51] P. Vasileva, B. Donkova, I. Karadova, C. Dushkin, Synthesis of starch-stabilized silver nanoparticles and their application as a surface plasmon resonance-based sensor of hydrogen peroxide, Colloids Surf. A 382 (2010) 203–210.
- [52] V. Kathiravan, S. Ravi, S. Ashokkumar, Synthesis of silver nanoparticles from *Melia dubia* leaf extract and their *in vitro* anticancer activity, Spectrochim. Acta A: Mol. Biomol. Spectrosc 130 (2014) 116–121.
- [53] A.K. Mittal, J. Bhaumik, S. Kumar, U.C. Banerjee, Biosynthesis of silver nanoparticles: elucidation of prospective mechanism and therapeutic potential, J. Colloid Interface Sci. 415 (2014) 39–47.
- [54] N.J. Reddy, D.N. Vali, M. Rani, S. Sudha Rani, Evaluation of antioxidant, antibacterial and cytotoxic effects of green synthesized silver nanoparticles by *Piper longum* fruit, Mater. Sci. Eng. C: Mater. Biol. Appl. 34 (2014) 115–122.
- [55] C. Dipankar, S. Murugan, The green synthesis, characterization and evaluation of the biological activities of silver nanoparticles synthesized from *Iresine herbstii* leaf aqueous extracts, Colloids Surf. B 98 (2012) 112–119.
- [56] M.S. Abdel-Aziz, M.S. Shaheen, A.A. El-Nekeety, M.A. Abdel-Wahhab, Antioxidant and antibacterial activity of silver nanoparticles biosynthesized using *Chenopodium murale* leaf extract, J. Saudi Chem. Soc. 18 (2014) 356–363.
- [57] L. Inbathamizh, T. Mekalai Ponnu, E. Jancy Mary, *In vitro* evaluation of antioxidant and anticancer potential of *Morinda pubescens* synthesized silver nanoparticles, J. Pharm. Res. 6 (1) (2013) 32–38.
- [58] T.V.M. Sreekanth, S. Ravikumar, In-Yong Eom, Green synthesized silver nanoparticles using *Nelumbo nucifera* root extract for efficient protein binding, antioxidant and cytotoxicity activities, J. Photochem. Photobiol. B 141 (2014) 100–105.
- [59] A. Rajan, V. Vilas, D. Philip, Catalytic and antioxidant properties of biogenic silver nanoparticles synthesized using *Areca catechu* nut, J. Mol. Liq. 207 (2015) 231–236.
- [60] L.S. Devi, S.R. Joshi, Ultrastructures of silver nanoparticles biosynthesized using endophytic fungi, J. Microsc. Ultrastruct. 3 (1) (2015) 29–37.
- [61] M.I. Sriram, S.B. Kanth, K. Kalishwaralal, S. Gurunathan, Antitumor activity of silver nanoparticles in Dalton's lymphoma ascites tumor model, Int. J. Nanomed. 5 (2010) 753–762.
- [62] J.P. Jacob, S. Finub, A. Narayanan, Synthesis of silver nanoparticles using *Piper longum* leaf extracts and its cytotoxic activity against Hep-2 cell line, Colloids Surf. B 91 (2012) 212–214.